

Exact quantum states for the diagonal Bianchi type IX model with negative cosmological constant

Robert Paternoga and Robert Graham

Fachbereich Physik, Universität-Gesamthochschule Essen, 45117 Essen, Germany

Quantum states of the diagonal Bianchi type IX model with *negative* cosmological constant Λ are obtained by transforming the Chern-Simons solution in Ashtekar's variables to the metric representation. We apply our method developed earlier for $\Lambda > 0$ and obtain five linearly independent solutions by using the complete set of topologically inequivalent integration contours in the required generalized Fourier-transformation. A caustic in minisuperspace separates two Euclidean regimes at *small* and *large* values of the scale parameter from a single classically interpretable Lorentzian regime in between, corresponding to the fact that classically these model-Universes recollapse. Just one particular solution out of the five we find gives a normalizable probability distribution on both branches of the caustic. However, in contrast to the case of positive cosmological constant, this particular solution neither satisfies the semi-classical no-boundary condition, nor does the special initial condition it picks out for $\hbar \rightarrow 0$ evolve into a classically interpretable Universe.

I. INTRODUCTION

Quantum gravity with a non-vanishing cosmological constant formulated in Ashtekar's spin-connection variables [1–5] has interesting physical states given by the exponential of the Chern-Simons functional [5–7] and appropriate transformations thereof. In order to elucidate the physical meaning of such states it is interesting to consider their restrictions to spatially homogeneous cosmological models. In a recent paper [8], henceforth quoted as [I], we considered the diagonal Bianchi IX models with positive cosmological constant from this point of view and found that five linearly independent physical states in the metric representation could be derived from the Chern-Simons functional. This set of solutions was found to be in one to one correspondence with the set of topologically different integration contours which exist for the generalized Fourier-transformation from the Ashtekar-representation to the metric representation. Due to the positivity of the cosmological constant the quantum states found in [I] describe an expanding (or collapsing) classically interpretable Lorentzian Universe at large scale parameters. On the other hand, at sufficiently small scale parameters the action defined by the exponent of the wavefunction becomes imaginary and can be associated only with a quantum mechanically allowed Euclidean Universe. The two "phases" are separated by a caustic surface in minisuperspace. It was found that only one of the five linearly independent states defines a normalizable probability distribution on this caustic, that this state satisfies the no-boundary condition of Hartle and Hawking [9,10] semi-classically for $\hbar \rightarrow 0$ (which means on scales large compared to the Planck scale), and that, again for $\hbar \rightarrow 0$, it picks out an initial condition which evolves into a classically interpretable Lorentzian Universe. For details and further literature we refer to [I].

It is now of interest to consider also what happens for negative cosmological constant, even though it seems very unlikely that our Universe has $\Lambda < 0$ (The age-problem resulting from recently measured high values of the Hubble-parameter [11] and the measured large age of globular star-clusters and also the observed high density of galaxies with large red-shifts seem to call for $\Lambda > 0$). Our motivation is rather to try the method of [I] for a model-Universe which recollapses, i.e. for which quantum-mechanically a classically interpretable Lorentzian evolution phase is bounded for small *and* large values of the scale parameter by Euclidean evolution phases. Therefore, we have to expect the appearance of two caustic surfaces in the minisuperspace of these models, one at small and the other at large scale parameter. Is there still a wavefunction, or are there even several, which give a normalizable probability distribution on these surfaces, and how are these wavefunctions related to the no-boundary state?

To answer these questions we apply in section II the method of [I] to obtain expressions for again five linearly independent physical states and identify the caustic surfaces in minisuperspace. In section III we determine the behavior of the absolute square of the wavefunctions on the caustic and identify a single physical state which gives a normalizable probability distribution in this way. In section IV we summarize our results. Within the narrow class of models we consider here they seem to rule out, with high probability, a classically evolving Universe with $\Lambda < 0$.

II. QUANTUM STATES GENERATED BY THE CHERN-SIMONS SOLUTION

In this section we want to construct solutions of the Wheeler-DeWitt equation for the diagonal Bianchi type IX model with a cosmological constant $\Lambda < 0$,

$$\left\{ \left[\hbar \partial_\alpha - \Phi_{,\alpha} \right] \left[\hbar \partial_\alpha + \Phi_{,\alpha} \right] - \left[\hbar \partial_+ - \Phi_{,+} \right] \left[\hbar \partial_+ + \Phi_{,+} \right] - \left[\hbar \partial_- - \Phi_{,-} \right] \left[\hbar \partial_- + \Phi_{,-} \right] + 3 (8\pi)^2 \Lambda e^{6\alpha} \right\} \Psi(\alpha, \beta_\pm; \Lambda) = 0, \quad (2.1)$$

$$\text{where } \Phi := 2\pi e^{2\alpha} \text{Tr } e^{2\beta} \quad \text{and} \quad \beta = (\beta_{ij}) := \text{diag} \left(\beta_+ + \sqrt{3} \beta_-, \beta_+ - \sqrt{3} \beta_-, -2\beta_+ \right). \quad (2.2)$$

In this notation ∂_+ and ∂_- denote derivatives with respect to the variables β_+ and β_- , respectively. By writing the Wheeler-DeWitt equation in the form (2.1) we have assumed a specific factor-ordering, which is suggested by a supersymmetric extension of the model [12–14]. A different factor-ordering is obtained by considering (2.1) with Φ replaced by $-\Phi$. In the present paper, as in [I], we will restrict ourselves to the factor-ordering as in (2.1), while a brief comment on the solutions in the second case $\Phi \rightarrow -\Phi$ is given in appendix A.

If the expression (2.2) for Φ is inserted into the Wheeler-DeWitt equation (2.1), the following more explicit form is obtained

$$\left\{ \frac{\hbar^2}{3\pi^2} \left[\frac{\partial^2}{\partial \alpha^2} - \frac{\partial^2}{\partial \beta_+^2} - \frac{\partial^2}{\partial \beta_-^2} \right] - \frac{2\hbar}{\pi} a^2 \text{Tr } e^{2\beta} + a^4 \text{Tr} \left(e^{4\beta} - 2e^{-2\beta} \right) + \Lambda a^6 \right\} \Psi(\alpha, \beta_\pm; \Lambda) = 0, \quad (2.3)$$

where we have introduced the mean scale factor $a := 2e^\alpha$. As in the case $\Lambda > 0$, solutions of (2.3) can be obtained by a transformation to the Ashtekar representation, where the Chern-Simons functional, restricted to the Bianchi type IX case, turns out to be an exact solution. Two of the Fourier integrals which occur in the transformation back to the metric representation can be carried out analytically without any loss of generality and afterwards the same one dimensional integral representation as in [I] is obtained:¹

$$\Psi(\kappa, \beta_\pm; \lambda) \propto \int_{\mathcal{C}} du \exp \left[\frac{1}{\lambda} f(\sin u; \kappa, \beta_\pm) \right], \quad (2.4)$$

$$\text{with} \quad f(z; \kappa, \beta_\pm) := 2\kappa^2 e^{-2\beta_+} \frac{z + \cosh(2\sqrt{3}\beta_-)}{1 - z^2} - z^2 + 2\kappa e^{2\beta_+} \left(z - \cosh(2\sqrt{3}\beta_-) \right) - \kappa e^{-4\beta_+}. \quad (2.5)$$

Here we have introduced the new variable κ and parameter λ

$$\kappa := \frac{1}{12} \Lambda a^2, \quad \lambda := \frac{\hbar \Lambda}{6\pi}, \quad (2.6)$$

thereby effectively reducing the number of parameters occurring in (2.4), and we shall also make use of the variables κ_j defined by

$$\kappa_j := \kappa e^{-\beta_j}, \quad (2.7)$$

where the β_j are the entries of the diagonal anisotropy matrix β . The integration contour \mathcal{C} in the integral-representation (2.4) can be chosen quite freely, as long as a sufficiently strong fall-off for the integrand and its u -derivatives at the borders $\partial\mathcal{C}$ of \mathcal{C} is guaranteed. The proportionality factor left open in (2.4) may depend on λ and will be fixed later.

While in the case $\Lambda > 0$ the curves of steepest *descent* of $\Re f$ were of interest, now, due to the different sign of Λ , the curves of steepest *ascent* lead to suitable integration contours. Moreover, new possibilities for the location of the saddle-points occur, which we classify as follows:

¹ Here, in contrast to [I], the *total* action, including the part which effects the similarity transformation between Ashtekar and metric variables, has been defined as the exponent of the integrand.

- By choosing $|\kappa|$ sufficiently small at fixed β_{\pm} , it is always possible to make all five saddle points of $f(z)$ lie on the real axis of the complex z -plane, defining the *Euclid I*-region of minisuperspace. Note, however, that the corresponding points in the u -plane of fig.1 (here $u = \arcsin z$) are real-valued only for $|z| \leq 1$, whereas real z -values with $|z| > 1$ are mapped into complex conjugate pairs of points on the axes $\Re u = \pm \frac{\pi}{2}$ and periodic repetitions thereof.
- Except for the case $\beta_{\pm} = 0$, where all five saddle-points are on the real z -axis, there is the possibility for two of the saddle-points to become complex in the z -plane, which defines the *Lorentzian regime*.
- For large values of $|\kappa|$ one always enters the *Euclid II* region, where again all five saddle-points of $f(z)$ become real-valued.

Some typical locations of the saddle-points in these different regimes of minisuperspace and the corresponding curves of steepest ascent are presented in fig.1.

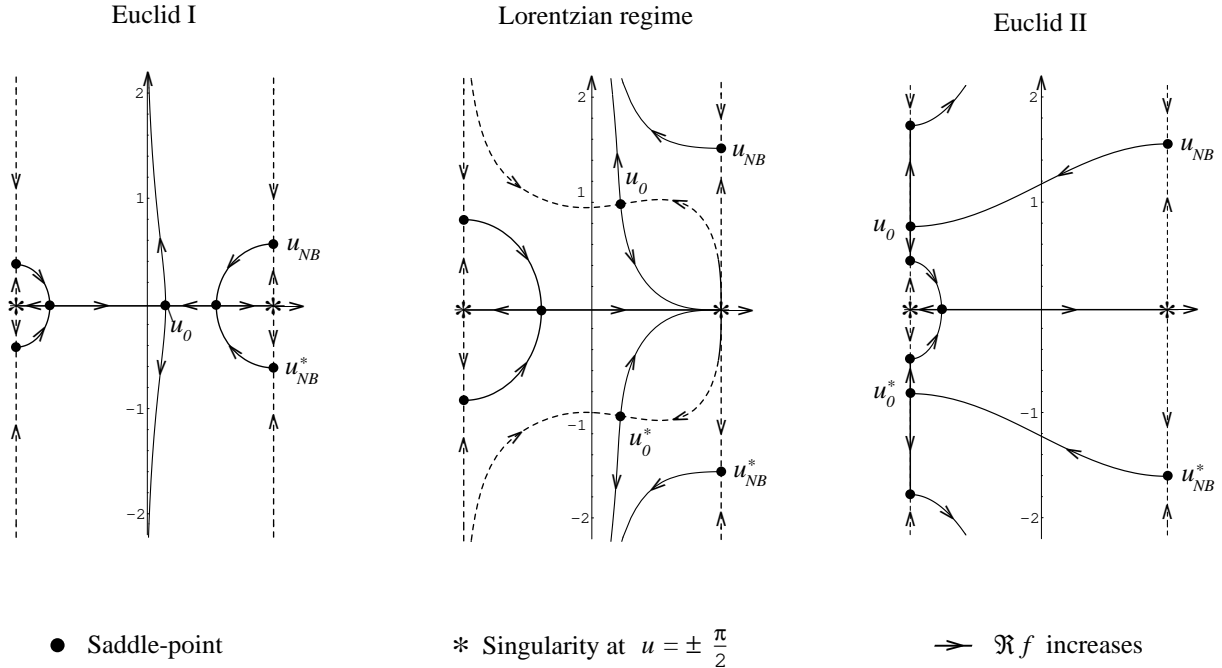


FIG. 1. Saddle-points and curves of steepest ascent of $\Re f$ in the complex u -plane for $\Lambda < 0$. The picture given in the Lorentzian case only holds for $\kappa_3 = \min\{\kappa_j\}$. The remaining case can easily be constructed by reflecting this figure on the imaginary axis. The dashed curves come from $-\infty$ with respect to $\Re f$ and are given just for completeness.

By passing from one of these regions to another, a *marginal* situation occurs, where two of the saddle-points conflate. We will refer to the corresponding hypersurface in minisuperspace as the *caustic*; it has been calculated and is plotted in fig.2. In contrast to the case $\Lambda > 0$ the caustic obtained here consists of an upper and a lower branch, which are connected just by a single *point* at $\kappa = -2$, $\beta_{\pm} = 0$. Furthermore, there are *kinks* at $\beta_+ > 0$, $\beta_- = 0$ and also at the other half-rays of the β_{\pm} -plane, related to the former by the typical β_{\pm} -symmetries of diagonal Bianchi IX.

Obviously, an exactly isotropic Universe $\beta_{\pm} = 0$ has to stay purely Euclidean throughout its evolution. On the other hand, “large” Universes with Lorentzian geometry must become very anisotropic. Apart from the possibility of a negative cosmological constant very close to zero, which would allow for large scale parameters even at $|\kappa|$ -values of order one, it seems impossible for the model under investigation to describe the Universe observed today.

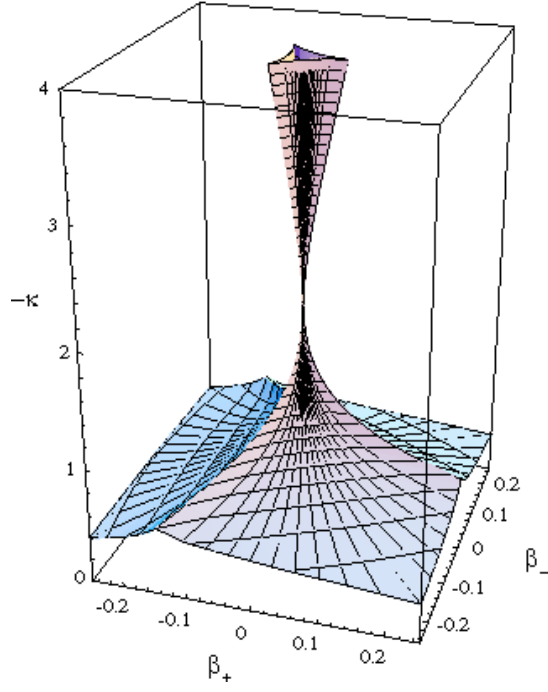


FIG. 2. The caustic in minisuperspace for $\Lambda < 0$

Nevertheless, let us now construct a basis of solutions to the Wheeler-DeWitt equation (2.3) by choosing topologically independent integration contours \mathcal{C} in the representation (2.4).

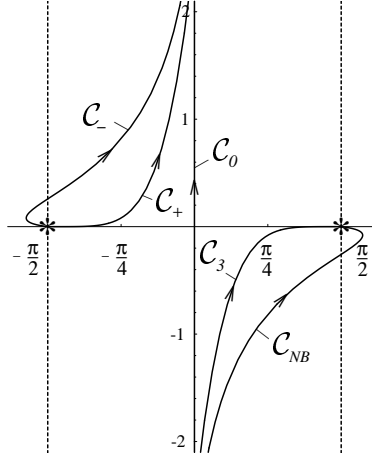


FIG. 3. Basis set of integration curves

Using the curves defined in fig.3 we introduce the following solutions

$$\Psi_0 := \frac{-i e^\mu}{K_0(-\mu)} \int_{\mathcal{C}_0} du \exp \left[\frac{1}{\lambda} f(\sin u) \right], \quad \Psi_\varrho := \frac{e^\mu}{\pi I_0(\mu)} \int_{\mathcal{C}_\varrho \oplus \mathcal{C}_\varrho^*} du \exp \left[\frac{1}{\lambda} f(\sin u) \right], \quad \varrho \in \{-, +, 3, NB\}, \quad (2.8)$$

$$\text{with} \quad \mu := \frac{1}{2\lambda}, \quad (2.9)$$

which, by definition, are real-valued and normalized in accordance with

$$\Psi_\varrho(a=0) \equiv 1 \quad , \quad \varrho \in \{0, -, +, 3, NB\} . \quad (2.10)$$

The functions K_0 and I_0 occuring in (2.8) are the usual modified Bessel functions with index 0. It will be of some advantage to replace the solutions Ψ_+ and Ψ_- by

$$\Psi_1 := \begin{cases} \Psi_+ , & \beta_- \geq 0 \\ \Psi_- , & \beta_- \leq 0 \end{cases} \quad , \quad \Psi_2 := \begin{cases} \Psi_+ , & \beta_- \leq 0 \\ \Psi_- , & \beta_- \geq 0 \end{cases} . \quad (2.11)$$

Then saddle-point expansions of the integrals (2.8) in the limit $\Lambda \rightarrow 0$, a and β_\pm fixed, reveal

$$\lim_{\Lambda \rightarrow 0} \Psi_0 = \Psi_{WH}^0 , \quad \lim_{\Lambda \rightarrow 0} \Psi_{NB} = \Psi_{NB}^0 , \quad \lim_{\Lambda \rightarrow 0} \Psi_i = \Psi_i^0 , \quad i \in \{1, 2, 3\} , \quad (2.12)$$

where the upper index “0” denotes the solutions of the $\Lambda = 0$ -model given in [I].

Without proof we mention that Ψ_i , $i \in \{1, 2, 3\}$, are three asymmetric solutions which generate each other by cyclic permutations of the κ_j , so consequently the sum of these states,

$$\Psi_\Sigma := \frac{1}{3} \sum_{i=1}^3 \Psi_i , \quad (2.13)$$

besides Ψ_0 and Ψ_{NB} , turns out to be symmetric with respect to arbitrary κ_j -permutations.

Up to different normalization factors, the asymptotic behavior in the limit $\kappa \rightarrow -\infty$ can immediately be extracted from the corresponding expansions in [I] by taking account of the negative sign of Λ . The only difficulty lies in the determination of the saddle-points, which give the dominating contribution to the different solutions in this limit. A detailed calculation finally yields

$$\Psi_0 \stackrel{\kappa \rightarrow -\infty}{\sim} \frac{\sqrt{\hbar}}{K_0(-\frac{3\pi}{\hbar\Lambda})} \left(-\frac{3}{\Lambda}\right)^{\frac{1}{4}} \left(\frac{a}{2}\right)^{-\frac{3}{2}} \exp\left[-\frac{\pi a^3}{\hbar} \sqrt{-\frac{\Lambda}{3}}\right] , \quad (2.14)$$

$$\Psi_{NB} \stackrel{\kappa \rightarrow -\infty}{\sim} \frac{\sqrt{\hbar}}{\pi I_0(\frac{3\pi}{\hbar\Lambda})} \left(-\frac{3}{\Lambda}\right)^{\frac{1}{4}} \left(\frac{a}{2}\right)^{-\frac{3}{2}} \exp\left[+\frac{\pi a^3}{\hbar} \sqrt{-\frac{\Lambda}{3}}\right] , \quad (2.15)$$

at $\beta_\pm = 0$, i.e. while Ψ_0 falls off rapidly for $a \rightarrow \infty$, the wavefunction Ψ_{NB} is strongly divergent in the same limit. Moreover, since Ψ_{NB} *always* gets its dominant contribution from the real saddle-point $z \geq 1$ (corresponding to the points u_{NB} and u_{NB}^* in the complex u -plane of fig.1 via $z = \sin u$), just Euclidean geometries are described by this state, so we will reject Ψ_{NB} as a physically relevant solution. Note, however, that it is the only state which satisfies the *no-boundary* condition in the limit $\hbar \rightarrow 0$, $a \rightarrow 0$, hence the name of this wavefunction.

To give the asymptotic behavior in the limit $\kappa \rightarrow -\infty$ for the states Ψ_i , $i \in \{1, 2, 3\}$, it will be helpful to consider

$$\Psi^i := \frac{1}{2} (\Psi_j + \Psi_k) , \quad \varepsilon_{ijk} = 1 , \quad (2.16)$$

instead. For these solutions the asymptotic expansions

$$\Psi^i \stackrel{\kappa \rightarrow -\infty}{\sim} -\frac{\Psi_{WH}^0}{I_0(\mu)} \sqrt{-\frac{\lambda}{\pi}} \frac{2}{\kappa_i} \left\{ 1 - 2 \frac{\kappa_j \kappa_k}{\kappa_i^3} \right\} \exp\left[\frac{1}{\lambda} \left(\kappa_i^2 - 2 \frac{\kappa_j \kappa_k}{\kappa_i} \right)\right] , \quad \varepsilon_{ijk} = 1 , \quad (2.17)$$

hold, so they fall off very rapidly for $a \rightarrow \infty$ (remember the negative sign of λ !).

By considering additional asymptotic expansions for large anisotropy it is possible to show that the four states Ψ_i , $i \in \{0, 1, 2, 3\}$, are all normalizable on minisuperspace in the distribution sense (see [I] for a discussion of this point for $\Lambda > 0$), i.e. so far we are left with a still four dimensional space of physically interesting solutions.

However, while in the Lorentzian regime Ψ_0 receives saddle-point contributions exclusively from the saddle-points at *complex* z and thus describes a Lorentzian Universe in this part of minisuperspace, the states Ψ_i , $i \in \{1, 2, 3\}$, get

additional Euclidean contributions of similar order of magnitude from *real* saddle-points and are therefore hard to interpret.

The classical trajectories which are generated by Ψ_0 in the semi-classical limit $\hbar \rightarrow 0$ in the *Lorentzian regime* can be computed by solving the equations

$$\frac{d\alpha}{dt} = -\frac{d\Im f(z_0)}{d\alpha}, \quad \frac{d\beta_{\pm}}{dt} = \frac{d\Re f(z_0)}{d\beta_{\pm}}, \quad (2.18)$$

where we have chosen the lapse-function to be $N = \frac{1}{2}\Lambda a^3$. While the complex saddle-point z_0 occurring in (2.18) is intended to correspond to the point u_0 of fig.1, the complex conjugate saddle-point $z_0^* = \sin u_0^*$, which describes the time-reversed classical evolution, can be considered with the same right. The corresponding second branch of the classical evolution of the Universe is actually *needed* to define the continuation of a classical trajectory which has reached the caustic: in approaching the caustic the saddle-points z_0 and z_0^* conflate and become real-valued, so that, in accordance with (2.18), the time-derivatives of α and β_{\pm} vanish. To continue such a trajectory in time, the time-reversed version of (2.18) has to be considered. Since the Universe is "reflected" in this way whenever it meets the caustic, and since in the generic case the classical trajectories have both of their endpoints on the caustic, *oscillating* Universes are described by Ψ_0 .

The numerical results for the classical trajectories which are obtained in the plane $\beta_- = 0$ of the minisuperspace are presented in fig.4.

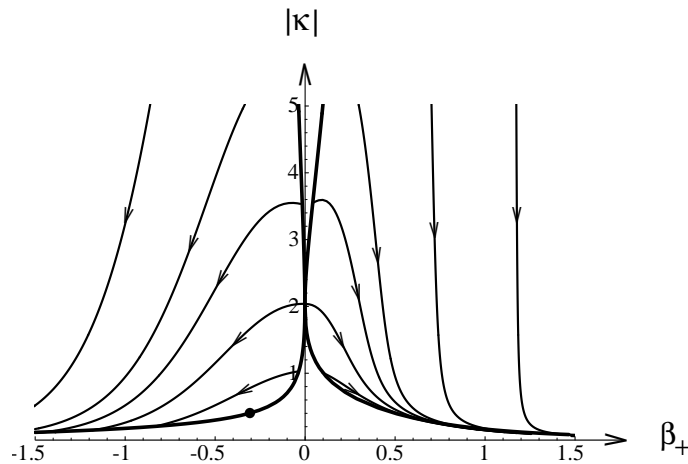


FIG. 4. Semi-classical trajectories generated by the complex saddle-points in the Lorentzian regime. For simplicity, we have restricted the plot to the plane $\beta_- = 0$. The arrows indicate the direction of increasing time t in eq. (2.18).

We should stress one important difference in the pictures which are obtained for the different signs of β_+ :

While for $\beta_+ > 0, \beta_- = 0$ all trajectories run to infinite anisotropy (which is, indeed, a peculiarity of the special β_{\pm} -direction, corresponding to a kink on the caustic, cf. fig.2), in the case $\beta_+ < 0$ the trajectories meet the lower branch of the caustic again at a finite β_+ -value, representing the general situation. This feature gives rise to the existence of a special trajectory with coinciding start- and endpoints, hence describing a Universe that never really becomes Lorentzian. The corresponding points in minisuperspace can be calculated analytically, requiring the solution of (2.18) to be *tangential* to the caustic, with the result

$$\kappa = -\sqrt[3]{2} \left(\frac{2}{5}\right)^{\frac{4}{3}}, \quad \beta_+ + i\beta_- = \frac{1}{6}(\ln 5 - 5 \ln 2) e^{\frac{2\pi i n}{3}}, \quad n \in \{-1, 0, 1\}. \quad (2.19)$$

These points will play an important role in the following section.

III. BEHAVIOR ON THE CAUSTIC

Since the classical Lorentzian evolution of the Universe described by the wavefunctions Ψ_i , $i \in \{0, 1, 2, 3\}$, is bounded by the caustic in minisuperspace, the value of $|\Psi|_c^2$ on the caustic predicted by the different solutions is of particular

interest. In fact $|\Psi|_c^2$ governs the realization of the different possible histories of the Universe and may thus be interpreted as the "initial" value distribution for the classical evolution.

However, at this stage a new problem arises due to the different branches of the caustic. Since the semi-classical trajectories always can be passed through in both directions, it is impossible to distinguish between their start- and endpoints. The distributions of $|\Psi|_c^2$ on the upper and lower branch of the caustic may therefore be considered with the same right, and we will always discuss them together in the following.

The numerical results obtained for $|\Psi_0|_c^2$ and $|\Psi_\Sigma|_c^2$ on the lower caustic are given in fig.5, and fig.6 shows the behavior on the upper caustic, which is very similar for the two different solutions. In the following the additional indices "u" and "l" denote the upper and lower branch of the caustic, respectively.

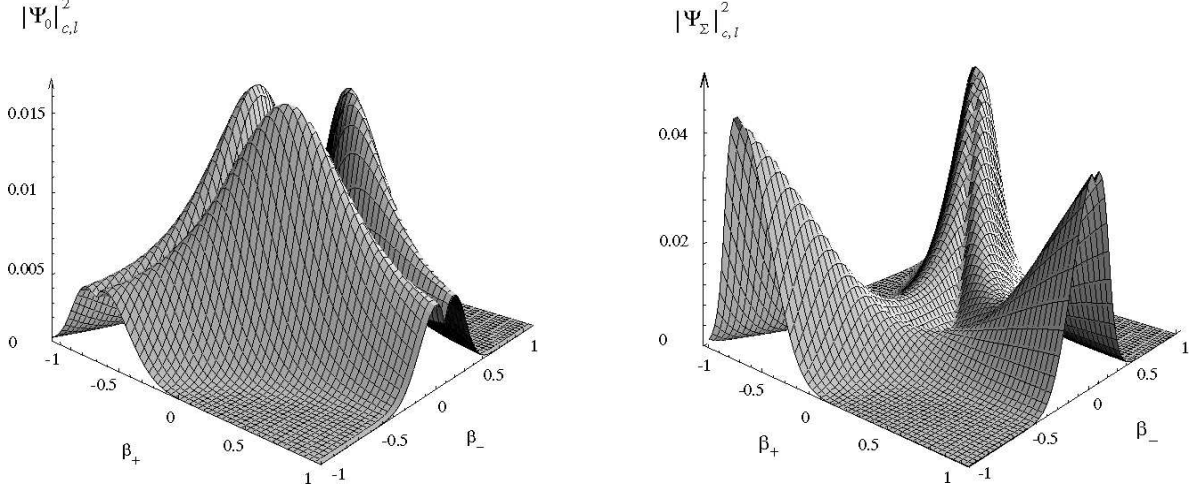


FIG. 5. Initial value distributions generated by Ψ_0 and Ψ_Σ on the lower caustic ($\Lambda = -3$, $\hbar = 2\pi$). Like the caustic itself, the distributions have kinks in some critical β_\pm -directions, which are partially hidden in the figures.

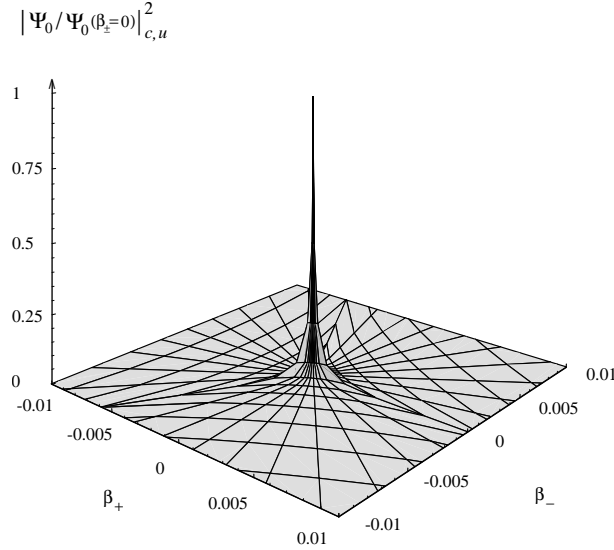


FIG. 6. Initial value distribution of Ψ_0 on the upper caustic, normalized to unity at $\beta_\pm = 0$. The numerical plots obtained for the different wavefunctions Ψ_0 and Ψ_Σ (and thus for $\hat{\Psi}$ defined below) on the upper caustic look very similar, so we restrict ourselves to a representation of $|\Psi_0|_{c,u}^2$. The absolute values taken by $|\Psi|_{c,u}^2$ at $\beta_\pm = 0$ are given by $1.45 \cdot 10^{-11}$, $3.56 \cdot 10^{-13}$ and $2.43 \cdot 10^{-11}$ for the wavefunctions Ψ_0 , Ψ_Σ and $\hat{\Psi}$, respectively (here again $\Lambda = -3$, $\hbar = 2\pi$). Since the lower and upper caustic coincide at $\beta_\pm = 0$, it is clear that these values hold for the distributions on the lower caustic, too. That is why we suggest to consider the two distributions obtained on the different branches of the caustic as analytical continuations of one another through the isotropic point.

While on the upper caustic both distributions fall off rapidly with increasing β_{\pm} and may be shown to be integrable over the β_{\pm} -plane, there are β_{\pm} -directions on the lower caustic, in which $|\Psi|_{c,l}^2$ approaches a finite value at infinity. Consequently, the wavefunctions on the lower branch are *not* square-integrable, and hence difficult to interpret as probability distributions. Nevertheless, as in the case $\Lambda > 0$, one may construct a new wavefunction as a linear combination of the two symmetric wavefunctions Ψ_0 and Ψ_{Σ} : By normalizing Ψ_0 and Ψ_{Σ} to approach unity in the critical β_{\pm} -directions, the difference of these new functions is square-integrable on the *full* caustic. To give an explicit expression for the quantum state obtained in this way, we introduce the integrals

$$\mathcal{J}_0^{(1)}(\nu) := \int_{-\frac{\pi}{4}}^{+\frac{\pi}{4}} dx e^{-\nu \sin^4 x}, \quad \mathcal{J}_0^{(2)}(\nu) := \int_{-\frac{\pi}{4}}^{+\frac{\pi}{4}} dx e^{-\nu \cos^4 x},$$

$$\mathcal{K}_0^{(1)}(\mu) := \int_0^{\infty} dt \sin(4\mu \sinh t) e^{\mu \cosh 2t}, \quad \mathcal{K}_0^{(2)}(\mu) := \int_0^{\infty} dt \cos(4\mu \sinh t) e^{\mu \cosh 2t}, \quad (3.1)$$

which, as far as we know, have no simple representation in terms of tabulated functions. Defining now

$$\mathcal{Q}(\lambda) := 3\pi e^{-3\mu} \frac{I_0(\mu)}{K_0(-\mu)} \frac{\mathcal{K}_0^{(2)}(\mu)}{2\mathcal{J}_0^{(1)}(8\mu) + \mathcal{J}_0^{(2)}(8\mu) + e^{-3\mu} \mathcal{K}_0^{(1)}(\mu)}, \quad \text{with } \mu = \frac{1}{2\lambda}, \quad (3.2)$$

the new state can be written in the form

$$\widehat{\Psi} := \frac{\Psi_0 - \mathcal{Q} \Psi_{\Sigma}}{1 - \mathcal{Q}}, \quad (3.3)$$

where the overall normalization factor has again been chosen to make $\widehat{\Psi} \equiv 1$ at $a = 0$. The behavior of $\widehat{\Psi}$ on the caustic has been computed for fig.7. Taking account of the full distribution, three maxima on the lower branch of the caustic pick out special initial values for the classical evolution of the Universe. The general representation (2.4) easily reveals that the wavefunction becomes arbitrarily sharply concentrated about these maxima in the limit $\lambda \rightarrow 0$, i.e. in particular in the limit $\hbar \rightarrow 0$ at fixed Λ . Consequently, in the semi-classical limit there are just three histories of the Universe which occur with significant probability.

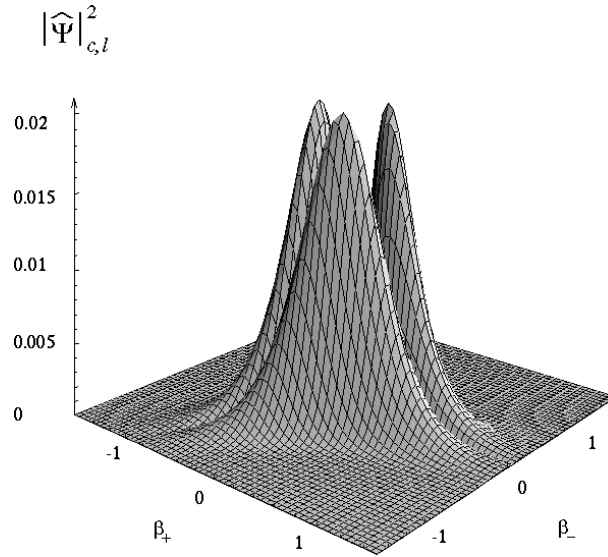


FIG. 7. Initial value distribution generated by $\widehat{\Psi}$ on the lower caustic ($\Lambda = -3$, $\hbar = 2\pi$). For the distribution obtained on the upper caustic see fig.6.

In the following we shall be interested in the special points of minisuperspace where the maxima of $|\widehat{\Psi}|_{c,l}^2$ arise. Using the saddle-point method for $\lambda \rightarrow 0$ the asymptotic behavior of the integrals defined in (3.1) after some calculation yields

$$\mathcal{Q} \xrightarrow{\lambda \rightarrow 0} \frac{3}{2} \sqrt{\frac{2}{\pi}} \Gamma(\frac{1}{4}) (-\lambda)^{-\frac{1}{4}} e^{\frac{3}{\lambda}}, \quad (3.4)$$

and with this result the relation

$$\widehat{\Psi} \stackrel{\hbar \rightarrow 0}{\sim} \Psi_0 \quad (3.5)$$

can be shown to hold at least on the lower caustic. Since $\widehat{\Psi}$ is a real-valued, non-vanishing wavefunction, the maxima of $|\widehat{\Psi}|^2$ coincide with the maxima of $\widehat{\Psi}$, and using (3.5) they may also be calculated from Ψ_0 in the semi-classical limit. By performing again a saddle-point expansion for $\lambda \rightarrow 0$, now in the integral representation (2.8) of Ψ_0 , the maxima of Ψ_0 on the caustic can be calculated analytically with the result given exactly by (2.19).

Consequently, within the class of solutions considered here, the *only* quantum state that is square-integrable on the full caustic turns out to predict a Universe which never becomes Lorentzian in the classical limit (albeit classical Lorentzian solutions of the Bianchi type IX model with negative cosmological constant actually do exist, cf. fig.4).

IV. CONCLUSION

In the present paper we constructed exact quantum states for the diagonal Bianchi type IX model with a negative cosmological constant. We found that the method presented in [I] for $\Lambda > 0$ is indeed perfectly applicable to the model with $\Lambda < 0$. As for $\Lambda > 0$ it gives five linearly independent solutions, which are generated by the Chern-Simons state using topologically different integration contours in the generalized Fourier-transformation to the metric representation. Imposing the condition that the wavefunction be normalizable on the caustic, just one wavefunction remains, that turns out to have some nice additional properties: It is found to be normalizable in minisuperspace in the distribution sense and it respects the symmetries of the Bianchi type IX model. However, this state does *not* satisfy the no-boundary condition in the semi-classical limit in contrast to the case $\Lambda > 0$, and it turns out to predict a Universe that never becomes Lorentzian, after all. Hence we obtain the result, that, *if* one allows for a non-zero cosmological constant at all, it should be positive, at least as far as the Chern-Simons functional related states of the quantized Bianchi IX model are concerned.

ACKNOWLEDGMENTS

Support of this work by the Deutsche Forschungsgemeinschaft through the Sonderforschungsbereich “Unordnung und große Fluktuationen” is gratefully acknowledged.

APPENDIX A: SOLUTIONS IN A DIFFERENT FACTOR-ORDERING

For completeness, and in order to obtain an important argument for the factor-ordering chosen for the Wheeler-DeWitt equation (2.3), we shall make some comments on a further class of solutions, which can again be discussed by using the methods of [I].

Considering the Wheeler-DeWitt equation in the form (2.1) one may ask, why we have not chosen a different factor-ordering, which is obtained by changing $\Phi \rightarrow -\Phi$. This choice, of course, would not have affected the classical Hamiltonian, but the quantum correction $-\frac{2\hbar}{\pi} a^2 \text{Tr} e^{2\beta}$ in (2.3) would have changed its sign.² Since the coordinate transformation $a \rightarrow i a, \Lambda \rightarrow -\Lambda$ has exactly the same effect as the above mentioned change of the factor-ordering, it is possible to discuss the solutions of the Wheeler-DeWitt equation in the new factor-ordering by considering still

²The factor-ordering obtained in this way corresponds to the \mathcal{A}^+ -representation introduced by Kodama in [6], in contrast to the \mathcal{A}^- -representation, which we have considered up to now.

equation (2.3), but substituting formally $a \rightarrow ia$, $\Lambda \rightarrow -\Lambda$ in the solutions. In the following it will be more convenient to use the coordinates κ_j and λ introduced in (2.6) and (2.7), which transform like $\kappa_j \rightarrow \kappa_j$, $\lambda \rightarrow -\lambda$ under this substitution.

It should be clear that the solutions of the Wheeler-DeWitt equation (2.3) are still of the form (2.4), but while we looked at the cases $\kappa > 0, \lambda > 0$ in [I] and $\kappa < 0, \lambda < 0$ in the present paper, now the remaining sectors $\kappa > 0, \lambda < 0$ and $\kappa < 0, \lambda > 0$ are of interest, which, because of the formal substitution $\lambda \rightarrow -\lambda$ just mentioned, describe solutions for *positive* and *negative* cosmological constant in the *new* factor-ordering, respectively. It is easily checked that the location of the saddle-points, and therefore the caustic, depends only on $f(z; \kappa, \beta_{\pm})$ defined in eq. (2.5). This means that, irrespective of the sign of λ , we deal with the caustic of [I] in the case $\kappa > 0$, and with the caustic fig.2 in the case $\kappa < 0$. On the other hand, it is just the sign of λ which decides whether the integration curves of [I] (for $\lambda > 0$) or of fig.3 (for $\lambda < 0$) give suitable integration contours.

However, constructing the solutions for the new factor-ordering in this manner and applying the saddle-point method to the integral representation (2.4) in the limit of large anisotropy β_{\pm} , it finally turns out, that *any* solution to the Wheeler-DeWitt equation in the new factor-ordering *diverges* for $\beta_{\pm} \rightarrow \infty$, at least in some β_{\pm} -sectors. In other words, in the new factor-ordering there is no solution which is normalizable in minisuperspace, not even in the distribution sense. Furthermore, if the behavior of the wavefunctions on the caustic is considered, actually none of these solutions is found to be square-integrable with respect to β_{\pm} .

Comparing these results with the nice normalizability properties of the solutions of the Wheeler-DeWitt equation in the factor-ordering of (2.1) presented in [I] and the present paper, we believe to have a compelling argument to rule out the new factor-ordering. It would be interesting if this argument could be extended even to the general, inhomogeneous case of quantum gravity.

-
- [1] A. Ashtekar, Phys. Rev. Lett. **57**, 2244 (1986); Phys. Rev. D **36**, 295 (1987)
 - [2] A. Ashtekar, in *Lectures on Nonperturbative Canonical Gravity* (World Scientific, Singapore 1991)
 - [3] A. Ashtekar, in *Polymer Geometry at the Planck Scale and the Quantum Einstein Equations*, electronic archive *hep-th/9601054*
 - [4] C. J. Isham, *Structural Issues in Quantum Gravity*, electronic archive *gr-qc/9510063*
 - [5] K. Ezawa, *Nonperturbative solutions for canonical quantum gravity: an overview*, electronic archive *gr-qc/9601050*
 - [6] H. Kodama, Phys. Rev. D **42**, 2548 (1990)
 - [7] M. P. Brenckow, Nucl. Phys. B **341**, 213 (1990)
 - [8] R. Graham and R. Paternoga, *Physical states of Bianchi type IX quantum cosmologies described by the Chern-Simons functional*, electronic archive *gr-qc/9603027*. This paper is quoted as [I].
 - [9] J. B. Hartle and S. W. Hawking, Phys. Rev. D **28**, 2960 (1983)
 - [10] S. W. Hawking, Nucl. Phys. B **239**, 257 (1984)
 - [11] W. Freedman et al., Nature **371**, 757 (1994)
 - [12] R. Graham, Phys. Rev. Lett. **67**, 1381 (1991)
 - [13] J. Bene and R. Graham, Phys. Rev. D **49**, 799 (1994)
 - [14] A. Csordás and R. Graham, Phys. Rev. Lett. **74**, 4129 (1995)